PACSIN2 accelerates nephrin trafficking and is up-regulated in diabetic kidney disease

Dumont, Vincent

2017-09

Dumont , V , Tolvanen , T A , Kuusela , S , Wang , H , Nyman , T A , Lindfors , S , Tienari , J , Nisén , H , Suetsugu , S , Plomann , M , Kawachi , H & Lehtonen , S 2017 , ' PACSIN2 accelerates nephrin trafficking and is up-regulated in diabetic kidney disease ' , FASEB Journal , vol. 31 . https://doi.org/10.1096/fj.201601265R

http://hdl.handle.net/10138/224309
https://doi.org/10.1096/fj.201601265R

The FASEB Journal article fj.201601265R. Published online May 26, 2017.

THE FASEB JOURNAL • RESEARCH • www.fasebj.org

PACSIN2 accelerates nephrin trafficking and is up-regulated in diabetic kidney disease

Vincent Dumont,* Tuomas A. Tolvanen,* Sara Kuusela,* Hong Wang,* Tuula A. Nyman,[†,1] Sonja Lindfors,* Jukka Tienari,*,[‡] Harry Nisen,[§] Shiro Suetsugu,[¶] Markus Plomann,[‖] Hiroshi Kawachi,[#] and Sanna Lehtonen*,[2]

*Department of Pathology and [†]Institute of Biotechnology, University of Helsinki, Helsinki, Finland; [‡]Department of Pathology, Helsinki University Hospital, Hyvinkää, Finland; [§]Department of Urology, Helsinki University Hospital, Helsinki, Finland; [¶]Graduate School of Biological Sciences, Nara Institute of Science and Technology, Ikoma, Japan; [‖]Center for Biochemistry, University of Cologne, Germany; and [#]Department of Cell Biology, Kidney Research Center, Niigata University Graduate School of Medical and Dental Sciences, Niigata, Japan

ABSTRACT: Nephrin is a core component of podocyte (glomerular epithelial cell) slit diaphragm and is required for kidney ultrafiltration. Down-regulation or mislocalization of nephrin has been observed in diabetic kidney disease (DKD), characterized by albuminuria. Here, we investigate the role of protein kinase C and casein kinase 2 substrate in neurons 2 (PACSIN2), a regulator of endocytosis and recycling, in the trafficking of nephrin and development of DKD. We observe that PACSIN2 is up-regulated and nephrin mislocalized in podocytes of obese Zucker Diabetic Fatty (ZDF) rats that have altered renal function. In cultured podocytes, PACSIN2 and nephrin colocalize and interact. We show that nephrin is endocytosed in PACSIN2-positive membrane regions and that PACSIN2 overexpression increases both nephrin endocytosis and recycling. We identify rabenosyn-5, which is involved in early endosome maturation and endosomal sorting, as a novel interaction partner of PACSIN2. Interestingly, rabenosyn-5 expression is increased in podocytes in obese ZDF rats, and, *in vitro*, its overexpression enhances the association of PACSIN2 and nephrin. We also show that palmitate, which is elevated in diabetes, enhances this association. Collectively, PACSIN2 is up-regulated and nephrin is abnormally localized in podocytes of diabetic ZDF rats. *In vitro*, PACSIN2 enhances nephrin turnover apparently *via* a mechanism involving rabenosyn-5. The data suggest that elevated PACSIN2 expression accelerates nephrin trafficking and associates with albuminuria.—Dumont, V., Tolvanen, T. A., Kuusela, S., Wang, H., Nyman, T. A., Lindfors, S., Tienari, J., Nisen, H., Suetsugu, S., Plomann, M., Kawachi, H., Lehtonen, S. PACSIN2 accelerates nephrin trafficking and is up-regulated in diabetic kidney disease. FASEB J. 31, 000–000 (2017). www.fasebj.org

KEY WORDS: endocytosis · recycling · rabenosyn-5 · palmitate · podocyte

Diabetic kidney disease (DKD), the renal complication of diabetes, accounts for 44% of all end-stage renal disease cases requiring renal transplantation in the United States (1). DKD occurs after decades of diabetes and is characterized by persistent albuminuria and declined glomerular filtration rate (GFR). The mechanisms underlying DKD are not fully elucidated, but injury of glomerular epithelial cells (podocytes) is involved. Podocytes participate in the ultrafiltration of plasma into urine together with the glomerular basement membrane (GBM) and endothelial cells. Podocytes are highly specialized cells, and their foot processes interdigitate with adjacent podocytes. The foot processes are connected by special cell-cell junctions called slit diaphragms. Nephrin is a key protein of the slit diaphragm, in which it functions both structurally and *via* its signaling capacity [reviewed by New *et al*. (2)]. Mutations in the nephrin gene, *NPHS1*, induce severe kidney failure due to expression of a truncated form of nephrin or defective trafficking of mutated nephrin to the plasma membrane (3, 4). Similarly, a mutation in *NPHS2*, encoding podocin, prevents efficient targeting of nephrin to the plasma membrane (5), where nephrin normally locates in caveolin-1–positive lipid rafts (6). This also results in defective renal function, which shows that localization of nephrin at the slit diaphragm is crucial.

ABBREVIATIONS: BAR, Bin-Amphiphysin-Rvs; BSA, bovine serum albumin; CIE, clathrin-independent endocytosis; CLC, clathrin light chain; CME, clathrin-mediated endocytosis; DKD, diabetic kidney disease; EE/SE, early/sorting endosomes; GBM, glomerular basement membrane; GFR, glomerular filtration rate; PACSIN, protein kinase C and casein kinase 2 substrate in neurons; PKC-α, protein kinase C α; PLA, proximity ligation assay; TIRF, total internal reflection fluorescence; ZDF, Zucker Diabetic Fatty

[1] Current affiliation: Department of Immunology, Institute of Clinical Medicine, University of Oslo and Rikshospitalet Oslo, Oslo, Norway.
[2] Correspondence: Department of Pathology, University of Helsinki, Haartmaninkatu 3, B241, FIN-00290 Helsinki, Finland. E-mail: sanna.h.lehtonen@helsinki.fi

doi: 10.1096/fj.201601265R
This article includes supplemental data. Please visit *http://www.fasebj.org* to obtain this information.

In DKD models, nephrin often appears to be downregulated (7, 8) or mislocalized (9). Nephrin participates in controlling the structure of podocyte foot processes and actin cytoskeleton *via* phosphorylation of its key tyrosine residues [reviewed by New *et al*. (2)]. Therefore, controlled trafficking of nephrin, and the subsequent coordinated signaling *via* nephrin, is essential for podocytes and glomerular permselectivity. Nephrin internalization occurs *via* clathrin-mediated endocytosis (CME) or the lipid raft pathway, one of the clathrin-independent endocytosis (CIE) pathways (10, 11). The choice between the pathways might be critical for glomerular function because the endocytic pathways have different dynamics and therefore apparently different impacts on nephrin signaling (11). However, the mechanisms underlying the trafficking of nephrin after its internalization remain largely unknown.

Protein kinase C and casein kinase 2 substrate in neurons 2 (PACSIN2), also known as syndapin II, is a member of the Bin-Amphiphysin-Rvs (BAR) family that contains an evolutionary membrane binding and sculpting domain. Specifically, PACSIN2 has an F-BAR domain, which induces negative curvature to membranes, and NPF motifs and an SH3 domain that bind to cytoskeletal, endocytic and recycling proteins (12, 13, 14). In kidney, PACSIN2 is expressed in tubules, where it participates in repair processes after ischemia-reperfusion injury (15). PACSIN2 is also present in podocytes (15), yet its function has remained uncharacterized. In this study, we investigate whether PACSIN2 regulates the trafficking of nephrin and whether PACSIN2 expression changes in DKD.

MATERIALS AND METHODS

Cell culture and preparation of cell lysates

Wild-type mouse podocytes and podocytes stably overexpressing nephrin were produced and maintained as described in Wasik *et al.* (16). Sodium palmitate (Sigma-Aldrich, St. Louis, MO, USA) was conjugated to free fatty acid-free bovine serum albumin (BSA) (Sigma-Aldrich) at a 3:1 molar ratio at 37°C for 1–2 h. When specified, medium was supplemented with 50 μM BSA-palmitate, and/or glucose concentration was increased from 25 to 40 mM. Similar concentrations of BSA and/or mannitol were used as controls. Cells were lysed in NP-40 or M-PER buffer (Thermo Fisher Scientific, Waltham, MA, USA) supplemented with inhibitors as previously described in Wasik *et al.* (16).

Metabolic measurements and tissue preparation of ZDF rats

Lean and obese male ZDF-Lepr^{fa}/Crt rats were purchased from Charles River Laboratories (Wilmington, MA, USA). Blood glucose was determined with Elite Glucometer (Bayer, Leverkusen, Germany). Serum and 24-h urine samples, collected in metabolic cages, were analyzed at the Biochemical Analysis Core for Experimental Research of the University of Helsinki using Advia 1650 (Siemens, Munich, Germany). The estimated GFR was calculated using the creatinine clearance method following the formula $C_{Cr} = (U_{Cr} \times V)/P_{Cr}$, where C_{Cr} is creatinine clearance (ml/min), U_{Cr} is urine creatinine (mg/ml), V is urine volume per min, and P_{Cr} is plasma creatinine (mg/ml). The result was adjusted to the weight of the rat. Glomerular fractions were isolated from kidney cortices by graded sieving (17) and lysed in NP-40 buffer. Freshly dissected kidney tissues were embedded in Tissue-Tek Optimum Cutting Temperature (OCT) compound (Sakura Finetek, Torrance, CA, USA) or fixed in 10% formalin followed by embedding in paraffin. The protocols were approved by the National Animal Experiment Board.

Human glomerular lysate preparation

Tissue was collected from the healthy part of the kidney from nephrectomy samples. Glomeruli were isolated by graded sieving with 425/250/150-μm sieves (Retsch, Haan, Germany) and lysed in M-PER buffer for coimmunoprecipitation. The use of human material was approved by The Hospital District of Helsinki and Uusimaa Medical Ethical Committee.

Antibodies

The antibodies used are listed in Supplemental Table 1.

Immunoperoxidase staining

Immunoperoxidase staining was performed as described in Wasik *et al.* (16), with an additional incubation at room temperature for 1 h prior to incubation over night at +4°C with anti-PACSIN2 IgG (P2P). Images of 15–24 glomeruli per rat (n = 6–8 per group) were taken by a researcher blinded to phenotype. Randomized images were scored from 0 (negative) to 5 (strong staining) by 2 researchers independently blinded to phenotype.

Immunoblotting

Podocyte and glomerular lysates were used for analyzing PACSIN2 (P2B), nephrin (Progen), and rabenosyn-5 expression levels as described in Lehtonen *et al.* (18) followed by quantification with the Odyssey Infrared Imaging System (Li-Cor Biosciences, Lincoln, NE, USA).

Indirect immunofluorescence

Kidney cryosections or cultured podocytes were stained as described in Heikkilä *et al.* (17). Samples were examined with SP8 or SP8 X confocal microscopes (Leica, Wetzlar, Germany). For nephrin granularity scoring, images of 8–10 glomeruli of 5–8 rats per group were taken by a researcher who was blinded to phenotype. Randomized images were scored from 0 (smooth) to 5 (granular) by 2 researchers independently based on the overall granularity of the nephrin staining, the presence of punctate accumulations, and the continuity of nephrin signal along the GBM.

Transient overexpression and knockdown

Mouse PACSIN2 cDNA (13) was subcloned into flag-containing pCMV-Tag2B (Stratagene; Agilent Technologies, Santa Clara, CA) or eGFP-N1 (Takara, Kusatsu, Japan) vectors using BamH1 restriction sites. Rabenosyn-5-eGFP plasmid was purchased from Addgene (Cambridge, MA, USA). Cells were transfected using Lipofectamine 2000 (Thermo Fisher Scientific) and used for experiments after 48 h.

Structured illumination microscopy

Podocytes overexpressing nephrin and PACSIN2-eGFP were incubated in complete medium containing nephrin 5-1-6 IgG conjugated with Attodye 647N (516-647N; see Supplemental Table 1) for 5 min, followed by surface-labeling with 516-647N on ice for 15 min and fixing with 4% paraformaldehyde at room temperature for 15 min. Images were acquired with a structured illumination microscopy system connected to an Eclipse Ti-E inverted microscope (Nikon, Tokyo, Japan) and the NIS-Elements advanced research v.4.5 software (Nikon).

Proximity ligation assay

Proximity ligation assay (PLA) was performed as previously described [referred to as Duolink *In Situ* by Wasik *et al*. (16)]. Single antibody reactions were used as negative controls.

Total internal reflection fluorescence microscopy

Podocytes were plated on glass-bottomed dishes and incubated in complete medium containing 516-647N. Images were acquired with a total internal reflection fluorescence (TIRF) microscopy system connected to an Eclipse Ti-E inverted microscope (Nikon) and the NIS-Elements advanced research v.4.5 software (Nikon).

On/In-Cell Western assay

Podocytes overexpressing nephrin were grown on 96-well plates and transfected with flag-PACSIN2 or empty vector. For On-Cell Western assay (Li-Cor Biosciences), cells were transferred onto ice and incubated with 5-1-6 IgG in PBS, 5% fetal bovine serum for 15 min. Cells were fixed with 4% paraformaldehyde at room temperature for 10 min, blocked in blocking buffer (Rockland, Pottstown, PA, USA), and incubated with IRDye 800 donkey anti-mouse IgG (Li-Cor Biosciences) in 1:1 mixture of Rockland blocking buffer-PBS, 0.1% Tween-20. Nuclear marker DRAQ5 (Thermo Fisher Scientific) was used for normalization. Detection and quantitation were performed with an Odyssey Infrared Imager (Li-Cor Biosciences). For In-Cell Western assay, cells were incubated with 5-1-6 IgG in complete medium for the indicated time and transferred onto ice for 15 min to allow binding of the antibody to nephrin newly exported to the plasma membrane. Cells were then processed as in On-Cell Western assay with an additional permeabilization with 0.1% Triton-X100 for 10 min.

Immunoprecipitation

Lysates were precleared with protein G-Sepharose (Thermo Fisher Scientific) and incubated with anti-PACSIN2, anti-rabenosyn-5 or purified rabbit IgG (Thermo Fisher Scientific) for 16 h at 4°C. Immune complexes were bound to rabbit TrueBlot beads (eBiosciences, San Diego, CA, USA), washed with M-PER buffer, and analyzed by mass-spectrometry or immunoblotted.

Protein identification by liquid chromatography-tandem mass spectrometry

Protein samples were analyzed by gel electrophoresis liquid chromatography-tandem mass spectrometry as previously described (19). The liquid chromatography-tandem mass spectrometry data were searched with in-house Mascot through ProteinPilot interface against the SwissProt database (UniProt; *http://www.uniprot.org/*.

Statistical analysis

The statistical significance was calculated by either Mann-Whitney U test when $n < 10$, or Student's t test when $n > 10$, using GraphPad v.6.02 software (GraphPad Software, La Jolla, CA, USA). Bars in the figures show the mean, and error bars show the SD.

RESULTS

PACSIN2 expression is elevated in podocytes of obese and diabetic ZDF rats

To investigate whether PACSIN2 expression level is changed in podocytes in DKD, we used Zucker Diabetic Fatty (ZDF) rats, which develop severe diabetes and renal defects (20). Eight-week-old ZDF rats served as a model of early loss of glomerular function, and 34-wk-old rats served as a model of advanced renal failure. As expected, the obese 34-wk-old ZDF rats displayed hyperglycemia,

TABLE 1. *Metabolic and renal parameters of 8- and 34-wk-old ZDF rats*

	8-wk-old ZDF rat		34-wk-old ZDF rat	
Variable	Lean (n = 7)	Obese (n = 7)	Lean (n = 8)	Obese (n = 6)
Weight (g)	222 ± 10	332 ± 28***	473 ± 20	412 ± 25***
Kidney weight (g)	1.04 ± 0.06	1.49 ± 0.12***	1.73 ± 0.12	2.55 ± 0.46***
6 h fasting blood glucose (mM)	5.97 ± 0.67	4.57 ± 0.80**	5.80 ± 0.72	30.97 ± 3.29***,[a]
24-h urine excretion (g)	2.9 ± 0.9	11.8 ± 4.4***	7.7 ± 1.5	42.9 ± 6.0***
24-h albumin excretion (μg)	55.0 ± 29.3	1660 ± 843***	234 ± 383	8336 ± 1171***
Urine albumin (mg/dl)/creatinine (g/dl) ratio	15.6 ± 9.1	307.3 ± 152.2***	15.2 ± 22.2	979.7 ± 153.5***
Urea nitrogen (mM)	5.17 ± 0.50	8.22 ± 1.31***	6.63 ± 1.09	9.76 ± 0.66**
Estimated GFR (ml/min/100 g)	0.274 ± 0.048	0.209 ± 0.021*	0.289 ± 0.085	0.195 ± 0.017*

[a]At 34 wk of age, the blood glucose level exceeded the maximum value of the glucometer in 2 obese rats for which the maximal value of the glucometer (33.3 mM) was given. *$P < 0.05$, **$P < 0.01$, ***$P < 0.001$.

declined estimated GFR, and severe albuminuria compared with lean controls (**Table 1**).

Analysis of kidney sections revealed elevated expression of PACSIN2 in glomeruli of both 8- and 34-wk-old obese rats compared with lean controls (**Fig. 1*A–C***). The staining pattern of PACSIN2 was typical for podocytes, surrounding the glomerular tuft, and particularly obvious in glomeruli of obese 34-wk-old rats (Fig. 1*A*, arrows). Western blotting of isolated glomeruli confirmed a trend of increased PACSIN2 expression at 8 wk and 90% increase at 34 wk in obese ZDF rats (Fig. 1*D–F*). Colocalization of PACSIN2 and nephrin appeared extended in glomeruli of 34-wk-old ZDF rats (Fig. 1*G*), supporting increased expression of PACSIN2 in podocytes in DKD, which is in line with the immunohistochemistry data in Fig. 1*A*. Collectively, our findings indicate that PACSIN2 is

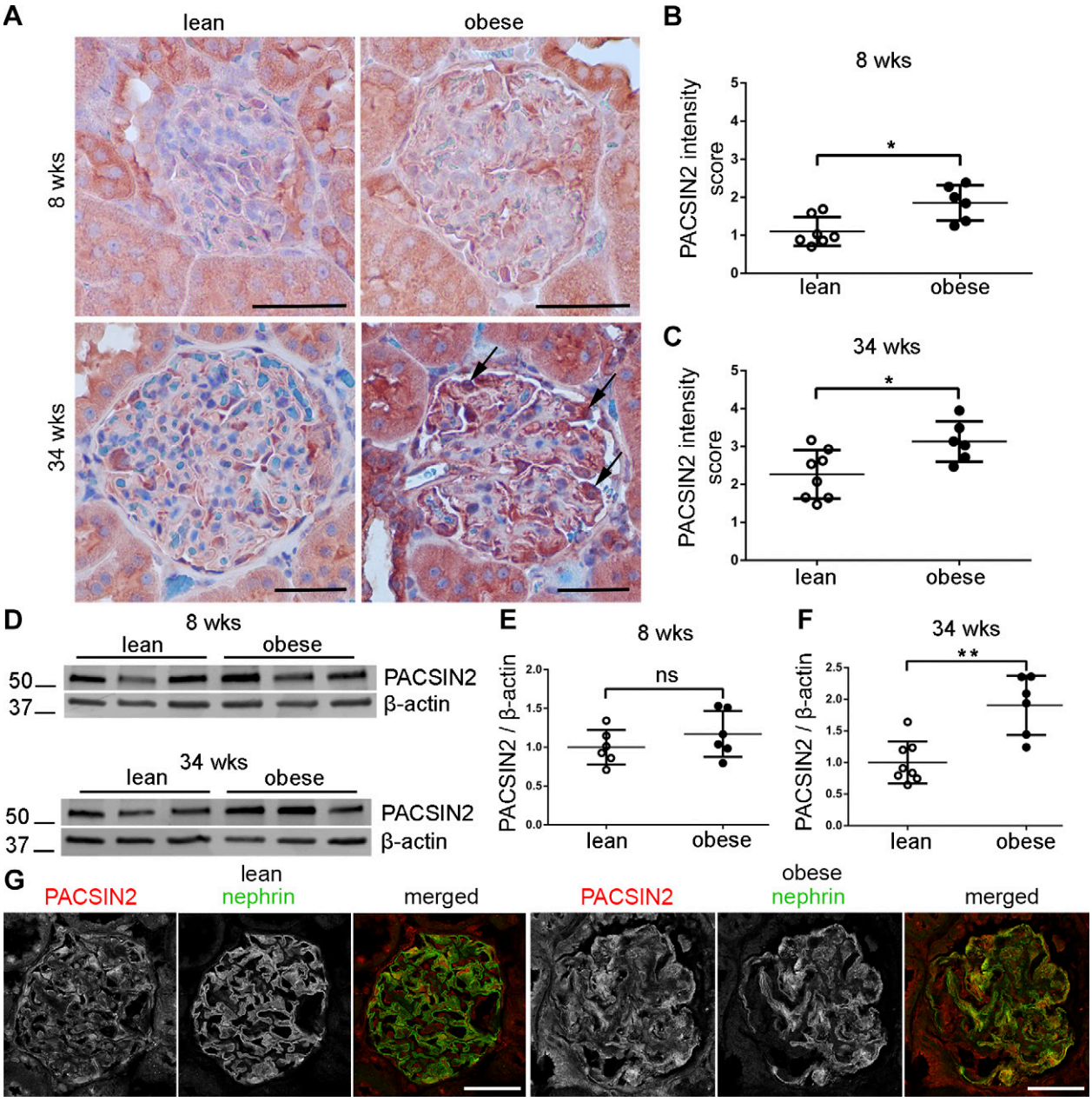

Figure 1. PACSIN2 expression level is increased in podocytes of obese ZDF rats. *A*) Immunohistological staining for PACSIN2 in kidney sections of lean and obese ZDF rats reveals elevated PACSIN2 levels in glomeruli of obese rats. Arrows pinpoint strong staining in cells, which exhibit the typical localization of podocytes in the outer part of the glomerular tuft. *B*, *C*) Scoring of PACSIN2 staining intensity in glomeruli of 8- (*B*) and 34–wk-old (*C*) ZDF rats, from 0 (negative) to 5 (strong staining). Each data point represents the average score of all glomeruli (15–24) analyzed in each rat ($n = 6–8$). At both 8 and 34 wk, glomeruli of obese rats showed elevated PACSIN2 staining compared with lean control rats. (*D*) Representative Western blot of PACSIN2 in lysates prepared of glomeruli isolated from 3 individual rats per group. β-actin is used as a loading control. *E*, *F*) Quantification of Western blots similar to *D* ($n = 6–8$ per group). A trend of increase in the expression of PACSIN2 is observed in the glomeruli of 8-wk-old obese rats compared with lean control rats (*E*). The increase is significant in glomeruli of 34-wk-old obese rats (*F*). *G*) Immunofluorescence staining reveals that at 34 wk, PACSIN2 and nephrin colocalize in the glomeruli of ZDF rats and that the colocalization appears extended in obese rats compared with lean control rats. Scale bars, 50 μm. Ns, nonsignificant. $*P < 0.05$, $**P < 0.01$.

up-regulated in podocytes of rats with diabetes and advanced renal defects.

Nephrin displays a granular localization in glomeruli of obese ZDF rats, but its expression level remains unchanged

Western blotting revealed no significant difference in the expression level of nephrin in the glomeruli of 8- or 34-wk-old rats (**Fig. 2*A*–*C***). However, the smooth appearance of nephrin staining as a continuous line along the GBM that was observed in lean rats was altered in the glomeruli of obese ZDF rats (Fig. 2*D*). Already at the age of 8 wk, irregularities in the staining pattern of nephrin along the GBM and occasional punctate accumulations were observed (Fig. 2*D*). At the age of 34 wk, abnormalities were clearer and more frequent, as a dotted line often replaced the smooth nephrin staining along the GBM. Grading of the granularity of nephrin staining revealed a clear trend at 8 wk and a significant increase at 34 wk (Fig. 2*E*, *F*).

To define the nature of nephrin aggregates, we performed double labelings of nephrin with vesicle trafficking

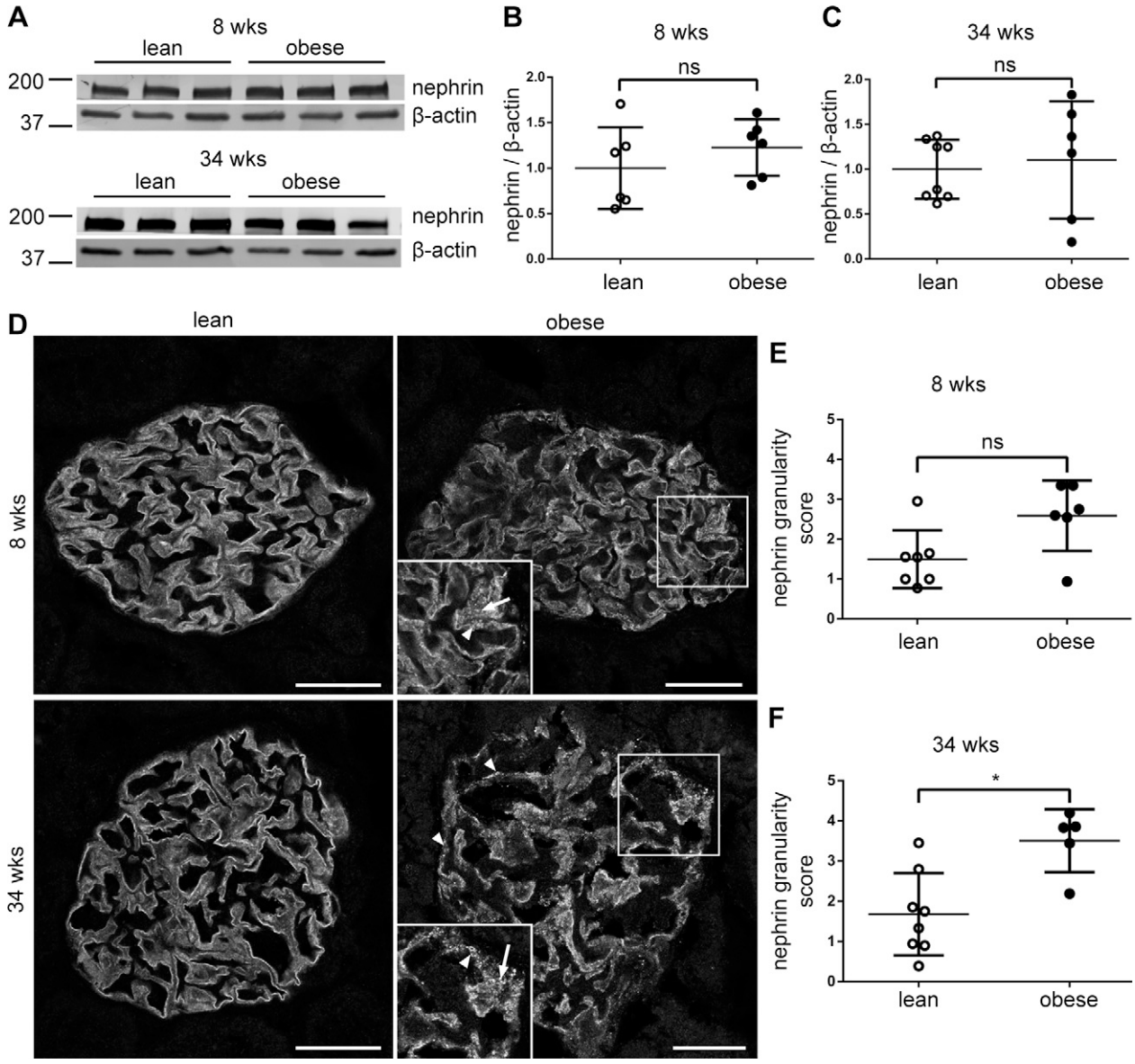

Figure 2. The expression level of nephrin in obese ZDF rats is unaffected, but its expression pattern becomes granular. *A*) Representative Western blots of nephrin in glomerular lysates from lean or obese rats at 8 or 34 wk of age ($n = 3$ per group). β-actin is used as a loading control. *B, C*) Quantification of immunoblots similar as in *A* ($n = 6$–8 per group). No difference in the expression level of nephrin is observed in the glomeruli of either 8- (*B*) or 34-wk-old (*B*) groups. *D*) Immunofluorescence images showing that in glomeruli of both 8- and 34-wk-old lean rats, the pattern of nephrin staining displays a smooth appearance with a sharp lining of the GBM. In glomeruli of obese rats, the staining for nephrin is irregular (arrowheads) and granules are occasionally observed (arrows). *E, F*) Scoring of the granularity of nephrin staining in glomeruli of 8- (*E*) and 34-wk-old (*F*) ZDF rats, from 0 (smooth pattern) to 5 (granular pattern). Each data point represents the average score of all glomeruli (8–10) analyzed in each rat ($n = 5$–8). At 8 wk, the granularity score of nephrin staining in glomeruli of obese rats is higher but did not reach statistical significance (*E*). At 34 wk, granularity of nephrin staining is significantly higher in obese rats compared to lean controls (*F*). Scale bars, 30 μm. Ns, nonsignificant. $^*P < 0.05$.

markers and slit diaphragm proteins. Clathrin heavy chain was found to partially colocalize with nephrin-positive punctate structures in glomeruli of obese 34-wk-old ZDF rats (Supplemental Fig. 1*A*). No significant colocalization of nephrin was observed with rab5, cathepsin D, or p62, which are markers of early endosomes, lysosomes, and autophagic cargo, respectively (Supplemental Fig. 1*B–D*). However, punctate accumulations of nephrin colocalized with the slit diaphragm proteins CD2AP and podocin, the latter showing a remarkably similar granular pattern as nephrin (Supplemental Fig. 1*E*, *F*). Collectively, in obese ZDF rats the expression pattern of nephrin becomes aberrant, although its expression level remains unchanged.

PACSIN2 and nephrin colocalize and interact *in vitro*

Using podocytes stably overexpressing nephrin, we observed that PACSIN2 and nephrin colocalize at the plasma membrane and on vesicles spread throughout the cytoplasm, including the leading edges and the perinuclear area (**Fig. 3*A***). This supports the hypothesis that PACSIN2 regulates several steps of nephrin trafficking. Next, we conjugated an antibody targeting the extracellular domain of nephrin (5-1-6 antibody) to a fluorophore, hereafter referred to as 516-647N. In podocytes overexpressing PACSIN2-eGFP, a 5-min pulse coupled with surface labeling of nephrin with 516-647N followed by high-resolution structured illumination microscopy confirmed the colocalization of PACSIN2 and nephrin at the plasma membrane and on early endocytic tubules (Fig. 3*B*, arrowheads). Moreover, PLA showed that endogenous PACSIN2 associates with nephrin (Fig. 3*C*).

PACSIN2 accelerates the trafficking of nephrin

To functionally assess whether PACSIN2 regulates nephrin endocytosis, we transiently overexpressed PACSIN2-eGFP in podocytes stably overexpressing nephrin and incubated the cells in complete medium containing 516-647N. Live TIRF microcopy videos revealed that nephrin is internalized at large and stable or small and versatile structures positive for PACSIN2-eGFP (**Fig. 4*A***) and Supplemental Video 1). Additionally, nephrin endocytosis was observed in areas devoid of PACSIN2-eGFP. We next transiently overexpressed fluorescently tagged caveolin-1 and clathrin light chain (CLC) in podocytes overexpressing nephrin and incubated podocytes with 516-647N for 20 min prior to fixation. TIRF microscopy revealed that nephrin occasionally colocalizes with both caveolin-1–DsRedmonomer and CLC-eGFP (Supplemental Fig. 2). This indicates that nephrin is present in both caveolin-1– and CLC-positive coated pits and suggests that it can be internalized *via* both CME and CIE. Also, colocalization of caveolin-1 and CLC with PACSIN2 supports that PACSIN2 regulates both CIE and CME (Supplemental Fig. 2).

To evaluate whether PACSIN2 regulates the presence of nephrin at the plasma membrane, we transiently overexpressed flag-PACSIN2 in podocytes overexpressing nephrin. PACSIN2 overexpression doubled the level of endogenous PACSIN2 without affecting the expression of nephrin (Supplemental Fig. 3*A–C*). On-Cell Western assay

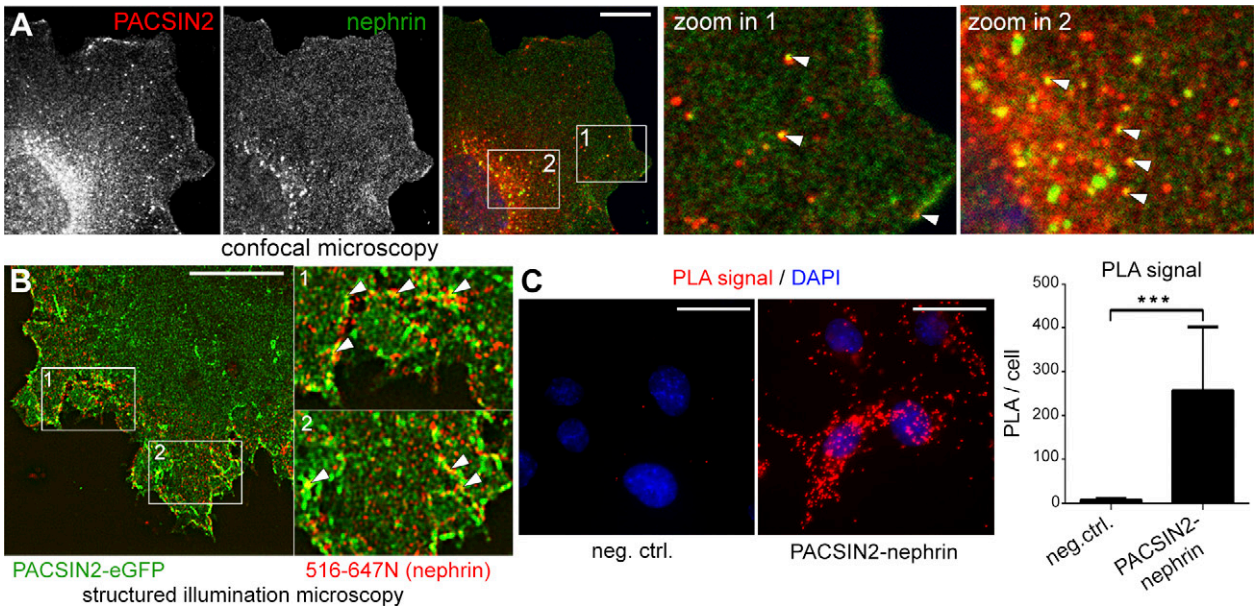

Figure 3. PACSIN2 colocalizes and associates with nephrin. *A*) Confocal microscopy shows colocalization of PACSIN2 and nephrin at the plasma membrane and on intracellular vesicles (arrowheads). *B*) High-resolution structured illumination microscopy of podocytes overexpressing PACSIN2-eGFP and pulsed with 516-647N for 5 min before surface labeling and fixation. Arrowheads indicate colocalization PACSIN2-eGFP and nephrin. *C*) Duolink PLA reveals that PACSIN2 and nephrin interact in mouse podocytes. PLA performed with nephrin 5-1-6 IgG alone is shown as a negative control. Total signal on microscope fields ($n = 8$), each containing 10–32 podocytes, was used for statistical analysis. Scale bars: 10 μm (*A*, *B*), 25 μm (*C*). ***$P < 0.001$.

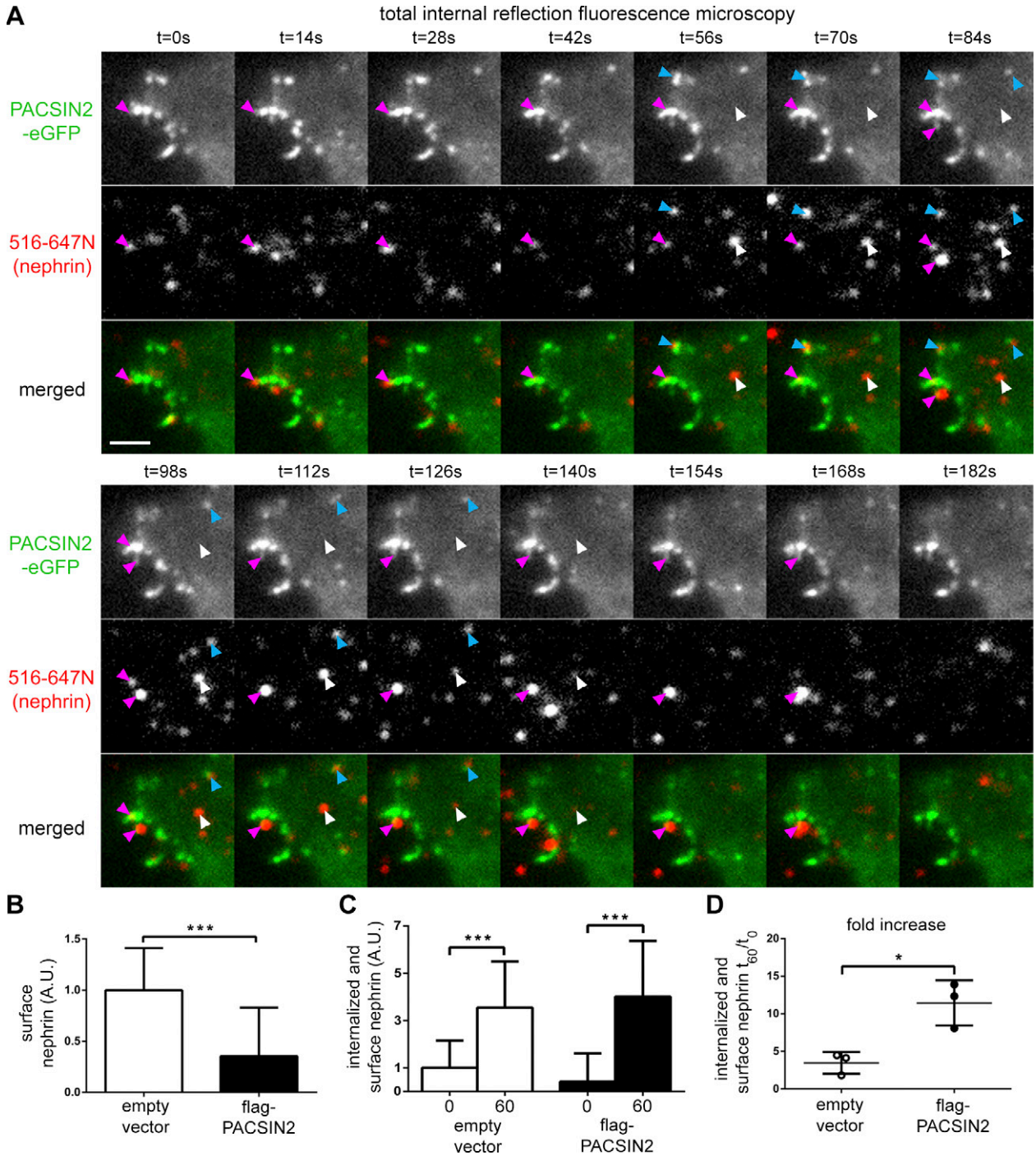

Figure 4. PACSIN2 enhances nephrin endocytosis and turnover. *A*) Live-cell TIRF microscopy analysis of podocytes overexpressing PACSIN2-eGFP and incubated with 516-647N reveals that nephrin undergoes endocytosis in PACSIN2-eGFP–positive spots. Arrowheads point to nephrin molecules which are internalized at either large and stable (magenta), or small and versatile (blue) PACSIN2-eGFP-positive spots. Arrowheads point at nephrin entering the cell in areas devoid of PACSIN2-eGFP. *B*) On-Cell Western analysis shows that overexpression of flag-PACSIN2 decreases the amount of nephrin inserted at the plasma membrane (n_{well} = 33–34). The results are expressed as arbitrary units, representing the intensity of nephrin staining normalized to the amount of cells measured using DRAQ5 staining intensity. *C*) In-Cell Western analysis indicates that both empty-vector and flag-PACSIN2 overexpressing podocytes have higher levels of nephrin stained after 60 min of incubation with the antibody followed by 15 min incubation on ice compared with the 15-min incubation on ice only (0 min), (n_{well} = 36). *D*) The ratio of nephrin stained at 60 and 0 min presented in *C* reveals that nephrin turnover at the plasma membrane is higher in flag-PACSIN2 overexpressing podocytes compared with empty vector -transfected cells. Each data point represents the average of a single experiment (n = 3) in *C*. Scale bar, 2 μm. $^*P < 0.05$, $^{***}P < 0.001$.

revealed that overexpression of flag-PACSIN2 reduced the amount of nephrin inserted at the plasma membrane by 65% (Fig. 4*B*). Next, we knocked down PASCIN2 using short interfering RNA. This increased the amount of nephrin inserted at the plasma membrane by 87% (Supplemental Fig. 3*F*), confirming that

PACSIN2 regulates the amount of nephrin present at the plasma membrane.

The reduction of nephrin at the plasma membrane observed in flag-PACSIN2–overexpressing podocytes could be due either to increased endocytosis of nephrin or slower delivery of nephrin to the plasma membrane. To distinguish between these options, we used an In-Cell Western assay approach in which 5-1-6 antibody was added to the culture medium of podocytes overexpressing flag-PACSIN2 or the empty vector for 0 or 60 min. Subsequently, surface-bound and internalized nephrin was detected as in On-Cell Western assay with an extra permeabilization step. At 0 min, less nephrin was detected in flag-PACSIN2–overexpressing podocytes than in empty vector–transfected cells (Fig. 4*C*), which is in line with Fig. 4*B*. Both empty vector– and flag-PACSIN2–transfected podocytes showed a strong increase of nephrin staining after 60 min (Fig. 4*C*), when slightly more nephrin was detected in the flag-PACSIN2–overexpressing podocytes compared with empty vector–transfected cells (+15%, nonsignificant) (Fig. 4*C*). This rules out the possibility that PACSIN2 overexpression prevents the delivery of nephrin to the plasma membrane. Strikingly, the ratio of stained nephrin at t_{60}/t_0, reflecting the increase of stained nephrin between 0 and 60 min, was significantly higher in flag-PACSIN2–overexpressing cells compared with empty vector–transfected cells (Fig. 4*D*). The significant increase in nephrin staining observed at 60 min suggests that internalized nephrin recycles back to the plasma membrane. This was confirmed by nephrin recycling assay (Supplemental Fig. 3*G*, *H*). Collectively, the data demonstrate that PACSIN2 overexpression accelerates both the endocytosis and recycling of nephrin, thereby enhancing nephrin turnover at the plasma membrane.

Rabenosyn-5 interacts with PACSIN2 and is up-regulated in podocytes of diabetic rats

To define the mechanisms by which PACSIN2 regulates nephrin trafficking, we searched for novel interaction partners of PACSIN2 in wild-type podocytes by immunoprecipitation of endogenous PACSIN2 followed by "shot-gun" mass spectrometry approach. Among the proteins identified, rabenosyn-5 (Mascot score, 45; $P < 0.05$) raised our interest because it has been shown to regulate the rate of endosomal recycling (21). Reciprocal coimmunoprecipitations confirmed that rabenosyn-5 and PACSIN2 form a complex in mouse podocytes overexpressing nephrin (**Fig. 5*A***) and isolated human glomeruli (Fig. 5*B*). Also, nephrin was observed in the precipitates, although its amount was fairly low (Fig. 5*A*, *B*). Western blotting revealed that the expression level of rabenosyn-5 was increased by 1.8- and 2.5-fold in glomeruli of obese ZDF rats compared with lean controls at both 8 and 34 wk, respectively (Fig. 5*C*–*E*). Immunofluorescence microscopy indicated an increase in rabenosyn-5 levels in glomeruli of 34-wk-old obese ZDF rats, and the expression pattern suggested an increase in podocytes and other glomerular cells (Fig. 5*F*).

Overexpression of rabenosyn-5 increases the association of nephrin with PACSIN2

Next, we overexpressed PACSIN2-eGFP or rabenosyn-5-eGFP in podocytes stably overexpressing nephrin followed by staining for endogenous rabenosyn-5 or PACSIN2, respectively. PACSIN2-eGFP appears to colocalize occasionally with both nephrin and rabenosyn-5 on intracellular vesicles all over the cytoplasm, concentrating close to the plasma membrane and in the perinuclear area (**Fig. 6*A***). Interestingly, overexpression of rabenosyn-5-eGFP led to a more vesicular localization pattern of PACSIN2 and nephrin in the juxtanuclear region and appeared to enhance the colocalization of the 3 proteins (Fig. 6*B*). To confirm this observation, we quantified the interaction between nephrin and PACSIN2 using PLA and found that the association of the 2 proteins increased by 90% in rabenosyn-5-eGFP–overexpressing podocytes compared with cells transfected with eGFP alone (Fig. 6*C*, *D*). The increase in complex formation is specific because neither PACSIN2 nor nephrin expression level was affected by rabenosyn-5-eGFP overexpression (Supplemental Fig. 4).

Palmitate enhances the association of nephrin with PACSIN2

To characterize which diabetes-associated circulating factor increases the association of PACSIN2 with nephrin and thereby potentially enhances the trafficking of nephrin, we treated podocytes with high glucose, palmitate, or a combination of the two and measured the association of nephrin and PACSIN2 by PLA. High glucose alone (40 mM, 48 h) did not increase the association of nephrin with PACSIN2. On the other hand, treatment of podocytes for 48 h with 50 μM palmitate enhanced their association by 27% and enhanced the combination of high glucose and palmitate by 32% (**Fig. 7**). The increase in complex formation was not due to increased expression of PACSIN2 or nephrin (Supplemental Fig. 5).

DISCUSSION

Despite intensive efforts, regulation of nephrin trafficking has remained unclear. Here, we demonstrate that the F-BAR protein PACSIN2 enhances nephrin endocytosis and recycling back to the plasma membrane. This apparently relies on the newly identified protein complex containing nephrin, PACSIN2 and rabenosyn-5, here identified in cultured podocytes and human glomeruli. Moreover, the formation of the PACSIN2-nephrin complex is enhanced by palmitate treatment.

PACSIN2 decreases the amount of nephrin at the plasma membrane, suggesting a role for PACSIN2 in nephrin endocytosis (Fig. 4). This is supported by the presence of PACSIN2-eGFP and nephrin on endocytic pits and early endosomal tubules (Figs. 3 and 4 and Supplemental Fig. 2). These results corroborate the ideas raised in previous studies, suggesting that nephrin endocytosis occurs *via* both CME and CIE (10, 11, 22, 23) and that

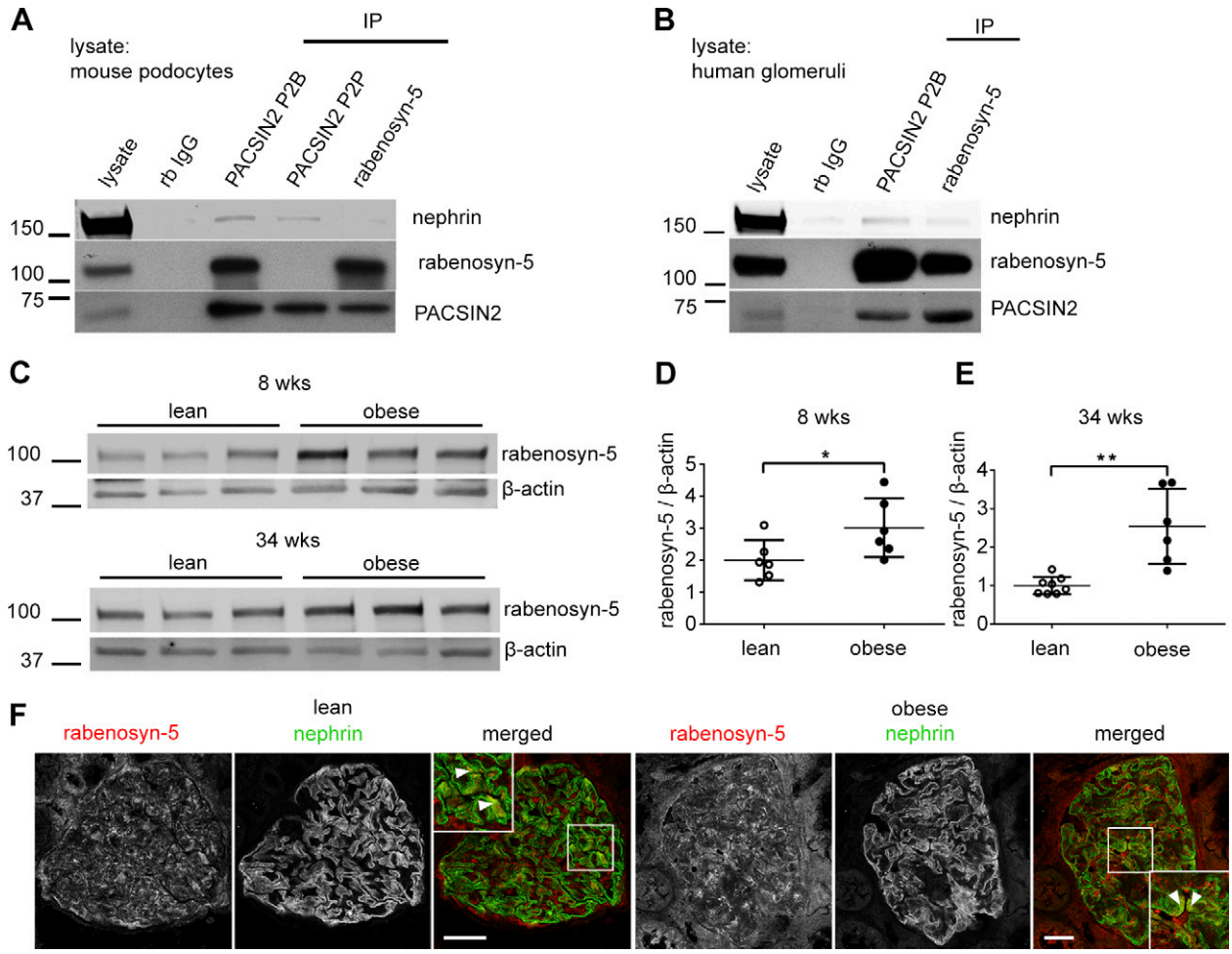

Figure 5. Rabenosyn-5 interacts with PACSIN2 and is increased in glomeruli of obese ZDF rats. *A*) Western blot showing that PACSIN2 and rabenosyn-5 coimmunoprecipitate in lysates of mouse podocytes overexpressing nephrin. Nephrin is also detected in PACSIN2 immunoprecipitations (IP). *B*) Western blot indicating that PACSIN2, rabenosyn-5 and nephrin coimmunoprecipitate in lysates of isolated human glomeruli. *C*) Representative Western blot of rabenosyn-5 in glomerular lysates from 3 individual rats per group. β-actin is included as a loading control. *D, E*) Quantification of the Western blots similar as in *C* (n = 6–8 per group). A 1.5-fold increase in the expression of rabenosyn-5 is observed in the glomeruli of 8 wk old rats and a 2.7-fold increase at the age of 34 wk (*D*) compared with lean controls (*E*). *F*) Immunofluorescence staining for rabenosyn-5 and nephrin in kidney sections of ZDF rats reveals that at 34 wk, the expression of rabenosyn-5 is increased in various glomerular cell types, including podocytes (arrowheads). Scale bars, 30 μm. $^*P < 0.05$, $^{**}P < 0.01$.

PACSIN2 regulates both CME and CIE (13, 14, 24). Interestingly, protein kinase C α (PKC-α), up-regulated in diabetic glomeruli (22, 23), is known to directly phosphorylate both nephrin and PACSIN2 (22, 23, 25). PKC-α–mediated phosphorylation of nephrin regulates its internalization (23), and the phosphorylation of PACSIN2 by PKC-α regulates caveolae-mediated endocytosis (25). Thus, PKC-α could be a major regulator of nephrin trafficking in diabetic conditions by a mechanism potentially involving PACSIN2. The fact that PKC-α deletion prevented the loss of nephrin expression in experimental DKD (26) further supports a role for PKC-α in the loss of kidney function in diabetes by regulating nephrin expression and trafficking. Taken together, our TIRF microscopy results and the results from previous studies demonstrate that nephrin internalization is complex and may occur *via* various pathways, some of which involve PACSIN2. The entry of nephrin into the cell may depend on whether nephrin is damaged or engaged in signaling or whether the glomeruli need to adapt to varying hemodynamic conditions.

Our study provides evidence that a significant amount of nephrin traffics back to the plasma membrane after internalization (Supplemental Fig. 3). This is in line with the idea that nephrin and other slit diaphragm components have a high turnover rate (27). We also show that PACSIN2 regulates not only endocytosis but also recycling of nephrin; both processes are necessary for accelerated turnover of nephrin at the plasma membrane (Fig. 4). This is supported by colocalization of PACSIN2 with nephrin in various intracellular locations (Fig. 3). Previous studies show that PACSIN2 localizes to early/sorting endosomes (EE/SE), tubular recycling endosomes, and the Golgi complex (28, 29). The novel interaction of PACSIN2 with rabenosyn-5 further supports a role for PACSIN2 in the recycling of nephrin. Rabenosyn-5 functions in EE/SE maturation and endosomal recycling as an effector of Rab5 and Rab4 (21, 30). Overexpression of rabenosyn-5 has been

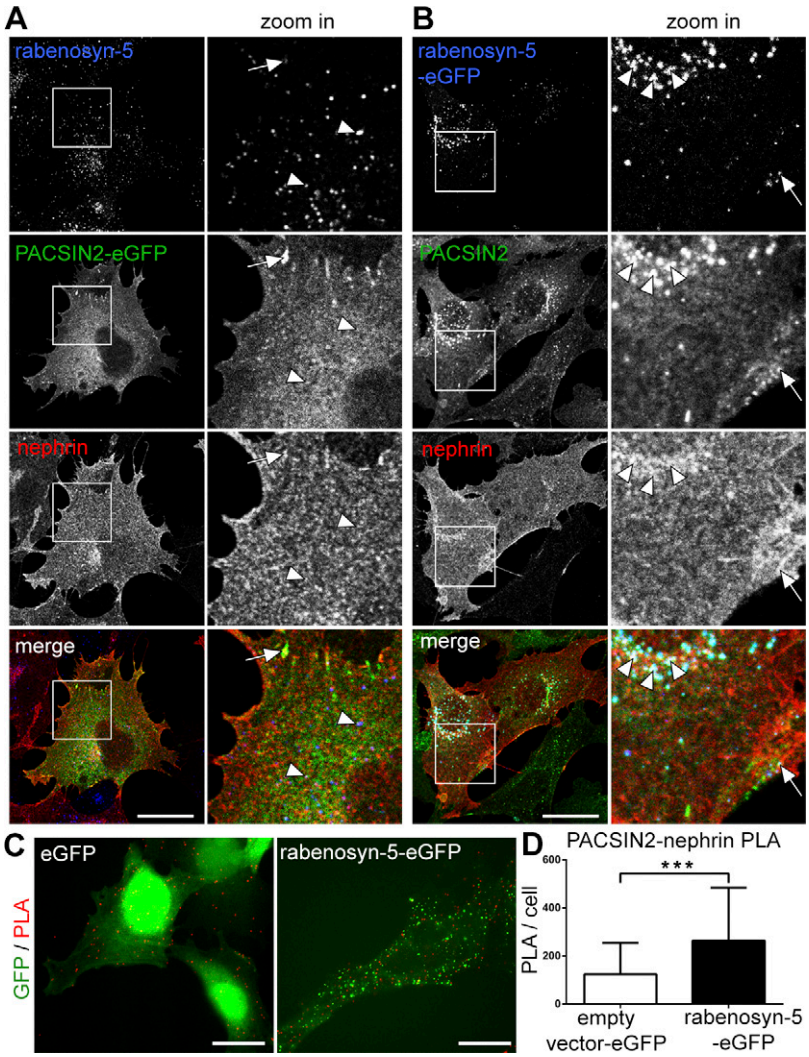

Figure 6. Rabenosyn-5 colocalizes with PACSIN2 and nephrin and increases their association. *A*) PACSIN2-eGFP overexpressed in podocytes colocalizes with rabenosyn-5 and nephrin near the plasma membrane (arrow) and on intracellular vesicles (arrowheads). *B*) Rabenosyn-5-eGFP overexpressed in podocytes colocalizes with PACSIN2 and nephrin at the cell edge (arrow) and on large juxtanuclear vesicles (arrowheads). *C*) PLA of PACSIN2 and nephrin in empty vector-eGFP and rabenosyn-5-eGFP overexpressing podocytes. *D*) Quantification of PLA signal as in (*C*) in individual podocytes overexpressing empty vector-eGFP or rabenosyn-5-eGFP ($n = 103–106$). Scale bars, 25 μm. $^{***}P < 0.001$.

shown to increase the size of the EE/SE compartment and to enhance the association of Rab4 and Rab5 and the recycling rate of transferrin (21). In podocytes with endogenous levels of rabenosyn-5, PACSIN2, nephrin, and rabenosyn-5 rarely colocalize (Fig. 6), suggesting that the interaction of the 3 proteins is transient in normal conditions (Figs. 5 and 6). However, overexpression of rabenosyn-5 attracted nephrin and PACSIN2 onto juxtanuclear vesicular structures and enhanced their association (Fig. 6). Further studies are required to characterize the interplay and shared function of PACSIN2 and rabenosyn-5 in podocytes. Previous work suggests that PACSIN2 is necessary for nucleation and scission of tubular recycling endosomes from rabenosyn-5–positive EE/SE (28, 31). Thus, their cooperation at the surface of endosomal membranes could contribute to changing the nature of maturing endosomes. Nonetheless, our results demonstrate a role for PACSIN2 in the recycling of nephrin, with a mechanism apparently involving rabenosyn-5. A role of rabenosyn-5 in the trafficking of nephrin could explain albuminuria observed in a patient who carries a mutated form of rabenosyn-5 (32).

In podocytes of obese and hyperglycemic ZDF rats, elevated expression of PACSIN2 and rabenosyn-5 is associated with a granular pattern of nephrin and severe albuminuria (Figs. 1, 2, and 5 and Table 1). The punctate structures positive for nephrin were occasionally also positive for clathrin heavy chain, highlighting a potential role for endocytosis in the pathophysiological changes occurring in podocytes in diabetic conditions. Previous electron microscopy studies reported that podocytes of obese ZDF rats present vacuolization and droplets and have an increased capacity for endocytosis (33, 34). We observed that endocytosed nephrin was not trapped in the endolysosomal system (Supplemental Fig. 2), but the punctate structures stained with antibodies against nephrin were also positive for CD2AP, which regulates intracellular trafficking in podocytes (35) and anchors the slit diaphragm to the cytoskeleton by binding actin directly (36). Strikingly, podocin, which escorts newly synthesized nephrin to the plasma membrane (5), also showed extensive colocalization with nephrin on the punctate structures (Supplemental Fig. 2). Therefore, one can speculate that podocin participates in the trafficking of nephrin in both health and disease, and that in diabetes the trafficking is aberrant, leading to the formation of vacuoles and aggregates. Protein and fat droplets have also been observed in podocytes of obese Zucker rats (37), a model of

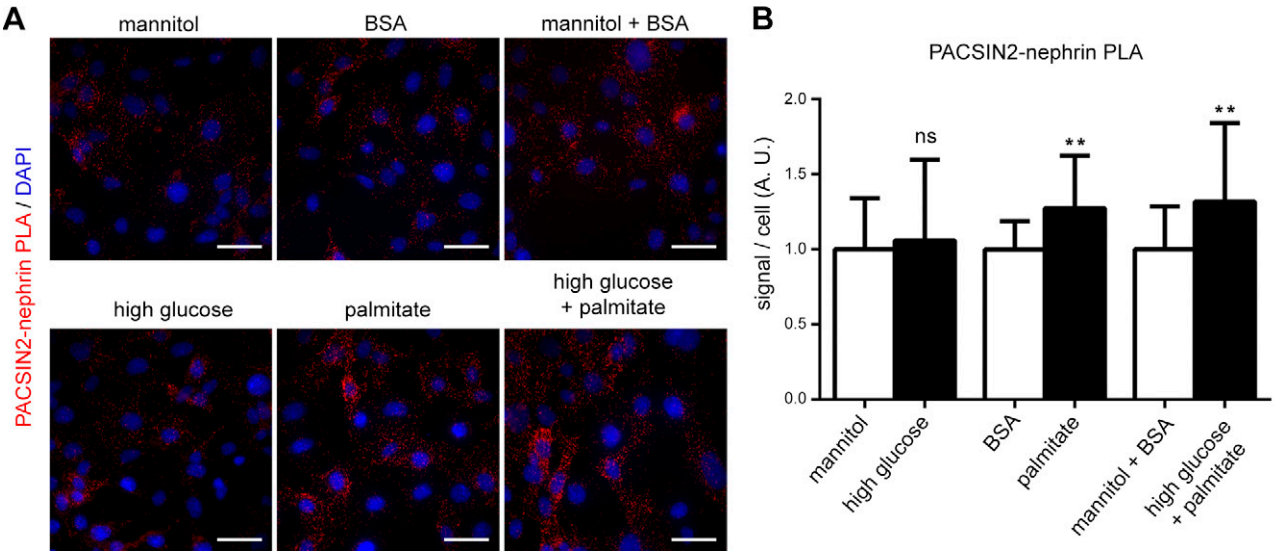

Figure 7. Stimulation of podocytes with palmitate enhances the association of nephrin with PACSIN2. *A*) PLA of PACSIN2 and nephrin in podocytes treated for 48 h with high glucose, palmitate or both high glucose and palmitate, as well as their respective controls. *B*) Quantification of PLA signal as in *A* shows that palmitate increases the association of nephrin with PACSIN2. Total signal on microscope fields ($n = 18$) was used for statistical analysis. Scale bars, 40 μm. Ns, nonsignificant. $^{**}P < 0.01$.

diabetes from which the ZDF rats originate. Interestingly, a recent study observed granular localization of nephrin and podocin in a protamine sulfate–induced podocyte effacement model (38), suggesting that abnormal trafficking of nephrin, along with podocin, is not limited to diabetes. It may be that in situations requiring fast glomerular adaptation, such as in diabetes and protamine-sulfate model, an increase in the turnover of the slit diaphragm proteins may lead to the saturation of the trafficking machinery, resulting in improper sorting and creation of aggregates containing nephrin and possibly other slit diaphragm components.

Palmitate, which is the most abundant free fatty acid (39), is elevated in the circulation of patients with insulin-resistant diabetes (40). Strikingly, both palmitate alone and in combination with high glucose led to an increase in the association of nephrin and PACSIN2 (Fig. 7). High glucose alone did not enhance the PACSIN2-nephrin association, possibly because a 48-h treatment was not long enough to mimic the constitutive metabolic pressure occurring in diabetes *in vivo*. This may also explain why the treatments did not change PACSIN2 expression level. Interestingly, palmitate enhances the activity of mTORC1 in podocytes (41), and constitutive activation of mTORC1 leads to aberrant localization of nephrin (9), reminiscent of the granular pattern of nephrin that we observed in ZDF rats. Previously, most studies have analyzed the expression level rather than the localization of nephrin in DKD and typically reported lower levels (7, 8, 26) or even up-regulation of nephrin (42). These discrepancies may be explained by the different models and methods used or the stage of disease analyzed.

In diabetes, glomeruli are subjected to hemodynamic stress (43), and podocytes must adapt to changing intraglomerular pressure to maintain the covering of the GBM. Thus, it is possible that up-regulation of PACSIN2 and rabenosyn-5 represents an adaptive mechanism aiming to maintain the integrity of the glomerular filtration barrier by increasing endocytosis and turnover of the slit diaphragm components, nephrin in particular. However, it remains to be analyzed whether PACSIN2 accelerates this turnover *in vivo* and whether accelerated trafficking of the slit diaphragm components prevents or worsens the development of DKD. Nonetheless, PACSIN2 may associate with renal pathophysiology, as suggested by our study and others. Indeed, PACSIN2 expression is elevated in proximal and collecting tubules in a model of ischemia-reperfusion injury, reflecting a potential role in tubulogenesis (15). In tubular cells, PACSIN2 also interacts with polycystin-1, which is mutated in polycystic kidney disease, further supporting a role for PACSIN2 in the maintenance of renal function (44).

In summary, we show here that PACSIN2, nephrin, and rabenosyn-5 form a complex in podocytes and propose that PACSIN2 fastens up the endocytosis and intracellular trafficking of nephrin by a mechanism involving rabenosyn-5. The elevated expression of PACSIN2 and rabenosyn-5 observed in DKD could reflect an attempt to adapt to the hemodynamic and metabolic stress, both deleterious for renal function. FJ

ACKNOWLEDGMENTS

The authors thank Dr. Andrey S. Shaw (Washington University School of Medicine, St. Louis, MO, USA) for the mouse podocyte cell line, and Dr. Silvia Corvera (University of Massachusetts Medical School, Worcester, MA, USA) for providing the rabenosyn-5 IgG; Dr. Yosuke Senju and Dr. Johan Peränen (both from the University of Helsinki) for fruitful discussions; Niina Ruoho and Leena Saikko (both from the University of Helsinki) for skillful technical assistance; and the Biomedicum Imaging Unit and Biochemical Analysis Core for Experimental Research of the University of Helsinki for help in imaging and metabolic measurements, respectively. This work was supported by the Academy of Finland (121248, 131255, 218021; to S.L.); the Sigrid

Juselius Foundation (to S.L.); the Päivikki and Sakari Sohlberg Foundation (to S.L.); the Diabetes Research Foundation (to S.L.); the Faculty of Medicine, University of Helsinki (to S.L.); the Research Foundation of the University of Helsinki (to V.D.); the Helsinki Biomedical Graduate Program (to V.D. and T.A.T.); the Finnish Cultural Foundation (to V.D.); the Helsinki University Hospital grant (to J.T.); and the Japan Society for the Promotion of Science (JSPS) Grant-in-Aid for Scientific Research (15H05902; to S.S.).

AUTHOR CONTRIBUTIONS

V. Dumont and S. Lehtonen designed the research; V. Dumont, T. A. Tolvanen, S. Kuusela, H. Wang, and T. A. Nyman performed the experiments; V. Dumont, T. A. Tolvanen, and S. Lehtonen analyzed the data; S. Lindfors, J. Tienari, H. Nisen, S. Suetsugu, M. Plomann, and H. Kawachi contributed material and new reagents; and V. Dumont and S. Lehtonen wrote the manuscript.

REFERENCES

1. Foley, R. N., and Collins, A. J. (2013) The USRDS: what you need to know about what it can and can't tell us about ESRD. *Clin. J. Am. Soc. Nephrol.* **8**, 845–851
2. New, L. A., Martin, C. E., and Jones, N. (2014) Advances in slit diaphragm signaling. *Curr. Opin. Nephrol. Hypertens.* **23**, 420–430
3. Kestilä, M., Lenkkeri, U., Männikkö, M., Lamerdin, J., McCready, P., Putaala, H., Ruotsalainen, V., Morita, T., Nissinen, M., Herva, R., Kashtan, C. E., Peltonen, L., Holmberg, C., Olsen, A., and Tryggvason, K. (1998) Positionally cloned gene for a novel glomerular protein–nephrin–is mutated in congenital nephrotic syndrome. *Mol. Cell* **1**, 575–582
4. Liu, L., Doné, S. C., Khoshnoodi, J., Bertorello, A., Wartiovaara, J., Berggren, P. O., and Tryggvason, K. (2001) Defective nephrin trafficking caused by missense mutations in the NPHS1 gene: insight into the mechanisms of congenital nephrotic syndrome. *Hum. Mol. Genet.* **10**, 2637–2644
5. Huber, T. B., Simons, M., Hartleben, B., Sernetz, L., Schmidts, M., Gundlach, E., Saleem, M. A., Walz, G., and Benzing, T. (2003) Molecular basis of the functional podocin-nephrin complex: mutations in the NPHS2 gene disrupt nephrin targeting to lipid raft microdomains. *Hum. Mol. Genet.* **12**, 3397–3405
6. Sörensson, J., Fierlbeck, W., Heider, T., Schwarz, K., Park, D. S., Mundel, P., Lisanti, M., and Ballermann, B. J. (2002) Glomerular endothelial fenestrae in vivo are not formed from caveolae. *J. Am. Soc. Nephrol.* **13**, 2639–2647
7. Bonnet, F., Cooper, M. E., Kawachi, H., Allen, T. J., Boner, G., and Cao, Z. (2001) Irbesartan normalises the deficiency in glomerular nephrin expression in a model of diabetes and hypertension. *Diabetologia* **44**, 874–877
8. Hyvönen, M. E., Dumont, V., Tienari, J., Lehtonen, E., Ustinov, J., Havana, M., Jalanko, H., Otonkoski, T., Miettinen, P. J., and Lehtonen, S. (2015) Early-onset diabetic E1-DN mice develop albuminuria and glomerular injury typical of diabetic nephropathy. *BioMed Res. Int.* **2015**, 102969
9. Inoki, K., Mori, H., Wang, J., Suzuki, T., Hong, S., Yoshida, S., Blattner, S. M., Ikenoue, T., Rüegg, M. A., Hall, M. N., Kwiatkowski, D. J., Rastaldi, M. P., Huber, T. B., Kretzler, M., Holzman, L. B., Wiggins, R. C., and Guan, K. L. (2011) mTORC1 activation in podocytes is a critical step in the development of diabetic nephropathy in mice. *J. Clin. Invest.* **121**, 2181–2196
10. Quack, I., Rump, L. C., Gerke, P., Walther, I., Vinke, T., Vonend, O., Grunwald, T., and Sellin, L. (2006) beta-Arrestin2 mediates nephrin endocytosis and impairs slit diaphragm integrity. *Proc. Natl. Acad. Sci. USA* **103**, 14110–14115
11. Qin, X. S., Tsukaguchi, H., Shono, A., Yamamoto, A., Kurihara, H., and Doi, T. (2009) Phosphorylation of nephrin triggers its internalization by raft-mediated endocytosis. *J. Am. Soc. Nephrol.* **20**, 2534–2545
12. Kessels, M. M., and Qualmann, B. (2004) The syndapin protein family: linking membrane trafficking with the cytoskeleton. *J. Cell Sci.* **117**, 3077–3086
13. Senju, Y., Itoh, Y., Takano, K., Hamada, S., and Suetsugu, S. (2011) Essential role of PACSIN2/syndapin-II in caveolae membrane sculpting. *J. Cell Sci.* **124**, 2032–2040
14. Modregger, J., Ritter, B., Witter, B., Paulsson, M., and Plomann, M. (2000) All three PACSIN isoforms bind to endocytic proteins and inhibit endocytosis. *J. Cell Sci.* **113**, 4511–4521
15. Yao, G., Luyten, A., Takakura, A., Plomann, M., and Zhou, J. (2013) The cytoplasmic protein Pacsin 2 in kidney development and injury repair. *Kidney Int.* **83**, 426–437
16. Wasik, A. A., Dumont, V., Tienari, J., Nyman, T. A., Fogarty, C. L., Forsblom, C., Lehto, M., Lehtonen, E., Groop, P. H., and Lehtonen, S. (2017) Septin 7 reduces nonmuscle myosin IIA activity in the SNAP23 complex and hinders GLUT4 storage vesicle docking and fusion. *Exp. Cell Res.* **350**, 336–348
17. Heikkilä, E., Ristola, M., Havana, M., Jones, N., Holthöfer, H., and Lehtonen, S. (2011) Trans-interaction of nephrin and Neph1/Neph3 induces cell adhesion that associates with decreased tyrosine phosphorylation of nephrin. *Biochem. J.* **435**, 619–628
18. Lehtonen, S., Lehtonen, E., Kudlicka, K., Holthofer, H., and Farquhar, M. G. (2004) Nephrin forms a complex with adherens junction proteins and CASK in podocytes and in madin-darby canine kidney cells expressing nephrin. *Am. J. Pathol.* **165**, 923–936
19. Savijoki, K., Lietzén, N., Kankainen, M., Alatossava, T., Koskenniemi, K., Varmanen, P., and Nyman, T. A. (2011) Comparative proteome cataloging of *Lactobacillus rhamnosus* strains GG and Lc705. *J. Proteome Res.* **10**, 3460–3473
20. Baynes, J., and Murray, D. B. (2009) Cardiac and renal function are progressively impaired with aging in Zucker diabetic fatty type II diabetic rats. *Oxid. Med. Cell. Longev.* **2**, 328–334
21. de Renzis, S., Sönnichsen, B., and Zerial, M. (2002) Divalent Rab effectors regulate the sub-compartmental organization and sorting of early endosomes. *Nat. Cell Biol.* **4**, 124–133
22. Tossidou, I., Teng, B., Menne, J., Shushakova, N., Park, J. K., Becker, J. U., Modde, F., Leitges, M., Haller, H., and Schiffer, M. (2010) Podocytic PKC-alpha is regulated in murine and human diabetes and mediates nephrin endocytosis. *PLoS One* **5**, e10185
23. Quack, I., Woznowski, M., Potthoff, S. A., Palmer, R., Königshausen, E., Sivritas, S., Schiffer, M., Stegbauer, J., Vonend, O., Rump, L. C., and Sellin, L. (2011) PKC alpha mediates beta-arrestin2-dependent nephrin endocytosis in hyperglycemia. *J. Biol. Chem.* **286**, 12959–12970
24. Taylor, M. J., Perrais, D., and Merrifield, C. J. (2011) A high precision survey of the molecular dynamics of mammalian clathrin-mediated endocytosis. *PLoS Biol.* **9**, e1000604
25. Senju, Y., Rosenbaum, E., Shah, C., Hamada-Nakahara, S., Itoh, Y., Yamamoto, K., Hanawa-Suetsugu, K., Daumke, O., and Suetsugu, S. (2015) Phosphorylation of PACSIN2 by protein kinase C triggers the removal of caveolae from the plasma membrane. *J. Cell Sci.* **128**, 2766–2780
26. Menne, J., Meier, M., Park, J. K., Boehne, M., Kirsch, T., Lindschau, C., Ociepka, R., Leitges, M., Rinta-Valkama, J., Holthofer, H., and Haller, H. (2006) Nephrin loss in experimental diabetic nephropathy is prevented by deletion of protein kinase C alpha signaling in-vivo. *Kidney Int.* **70**, 1456–1462
27. Satoh, D., Hirose, T., Harita, Y., Daimon, C., Harada, T., Kurihara, H., Yamashita, A., and Ohno, S. (2014) aPKCλ maintains the integrity of the glomerular slit diaphragm through trafficking of nephrin to the cell surface. *J. Biochem.* **156**, 115–128
28. Giridharan, S. S., Cai, B., Vitale, N., Naslavsky, N., and Caplan, S. (2013) Cooperation of MICAL-L1, syndapin2, and phosphatidic acid in tubular recycling endosome biogenesis. *Mol. Biol. Cell* **24**, 1776–1790, S1–S15
29. Billcliff, P. G., Noakes, C. J., Mehta, Z. B., Yan, G., Mak, L., Woscholski, R., and Lowe, M. (2016) OCRL1 engages with the F-BAR protein pacsin 2 to promote biogenesis of membrane-trafficking intermediates. *Mol. Biol. Cell* **27**, 90–107
30. Nielsen, E., Christoforidis, S., Uttenweiler-Joseph, S., Miaczynska, M., Dewitte, F., Wilm, M., Hoflack, B., and Zerial, M. (2000) Rabenosyn-5, a novel Rab5 effector, is complexed with hVPS45 and recruited to endosomes through a FYVE finger domain. *J. Cell Biol.* **151**, 601–612
31. Xie, S., Bahl, K., Reinecke, J. B., Hammond, G. R., Naslavsky, N., and Caplan, S. (2016) The endocytic recycling compartment maintains cargo segregation acquired upon exit from the sorting endosome. *Mol. Biol. Cell* **27**, 108–126
32. Stockler, S., Corvera, S., Lambright, D., Fogarty, K., Nosova, E., Leonard, D., Steinfeld, R., Ackerley, C., Shyr, C., Au, N., Selby, K., van Allen, M., Vallance, H., Wevers, R., Watkins, D., Rosenblatt, D., Ross, C. J., Conibear, E., Wasserman, W., and van Karnebeek, C.

(2014) Single point mutation in rabenosyn-5 in a female with intractable seizures and evidence of defective endocytotic trafficking. *Orphanet J. Rare Dis.* **9**, 141
33. Hoshi, S., Shu, Y., Yoshida, F., Inagaki, T., Sonoda, J., Watanabe, T., Nomoto, K., and Nagata, M. (2002) Podocyte injury promotes progressive nephropathy in zucker diabetic fatty rats. *Lab. Invest.* **82**, 25–35
34. Ina, K., Kitamura, H., Tatsukawa, S., Takayama, T., and Fujikura, Y. (2002) Glomerular podocyte endocytosis of the diabetic rat. *J. Electron Microsc.* **51**, 275–279
35. Tolvanen, T. A., Dash, S. N., Polianskyte-Prause, Z., Dumont, V., and Lehtonen, S. (2015) Lack of CD2AP disrupts Glut4 trafficking and attenuates glucose uptake in podocytes. *J. Cell Sci.* **128**, 4588–4600
36. Lehtonen, S., Zhao, F., and Lehtonen, E. (2002) CD2-associated protein directly interacts with the actin cytoskeleton. *Am. J. Physiol. Renal Physiol.* **283**, F734–F743
37. Coimbra, T. M., Janssen, U., Gröne, H. J., Ostendorf, T., Kunter, U., Schmidt, H., Brabant, G., and Floege, J. (2000) Early events leading to renal injury in obese Zucker (fatty) rats with type II diabetes. *Kidney Int.* **57**, 167–182
38. Subramanian, B., Sun, H., Yan, P., Charoonratana, V. T., Higgs, H. N., Wang, F., Lai, K. M., Valenzuela, D. M., Brown, E. J., Schlöndorff, J. S., and Pollak, M. R. (2016) Mice with mutant Inf2 show impaired podocyte and slit diaphragm integrity in response to protamine-induced kidney injury. *Kidney Int.* **90**, 363–372
39. Hagenfeldt, L., Wahren, J., Pernow, B., and Räf, L. (1972) Uptake of individual free fatty acids by skeletal muscle and liver in man. *J. Clin. Invest.* **51**, 2324–2330
40. Fraze, E., Donner, C. C., Swislocki, A. L., Chiou, Y. A., Chen, Y. D., and Reaven, G. M. (1985) Ambient plasma free fatty acid concentrations in noninsulin-dependent diabetes mellitus: evidence for insulin resistance. *J. Clin. Endocrinol. Metab.* **61**, 807–811
41. Yasuda, M., Tanaka, Y., Kume, S., Morita, Y., Chin-Kanasaki, M., Araki, H., Isshiki, K., Araki, S., Koya, D., Haneda, M., Kashiwagi, A., Maegawa, H., and Uzu, T. (2014) Fatty acids are novel nutrient factors to regulate mTORC1 lysosomal localization and apoptosis in podocytes. *Biochim. Biophys. Acta* **1842**, 1097–1108
42. Ku, C. H., White, K. E., Dei Cas, A., Hayward, A., Webster, Z., Bilous, R., Marshall, S., Viberti, G., and Gnudi, L. (2008) Inducible overexpression of sFlt-1 in podocytes ameliorates glomerulopathy in diabetic mice. *Diabetes* **57**, 2824–2833
43. Hostetter, T. H., Troy, J. L., and Brenner, B. M. (1981) Glomerular hemodynamics in experimental diabetes mellitus. *Kidney Int.* **19**, 410–415
44. Yao, G., Su, X., Nguyen, V., Roberts, K., Li, X., Takakura, A., Plomann, M., and Zhou, J. (2014) Polycystin-1 regulates actin cytoskeleton organization and directional cell migration through a novel PC1-Pacsin 2-N-Wasp complex. *Hum. Mol. Genet.* **23**, 2769–2779

Received for publication November 23, 2016.
Accepted for publication May 1, 2017.

PACSIN2 accelerates nephrin trafficking and is up-regulated in diabetic kidney disease

Vincent Dumont, Tuomas A. Tolvanen, Sara Kuusela, et al.

FASEB J published online May 26, 2017
Access the most recent version at doi:10.1096/fj.201601265R

Supplemental Figure legends

Supplemental Figure S1. Nephrin colocalizes with podocin, CD2AP and occasionally with clathrin but not with rab5, cathepsin D or p62 in the punctate structures in the ZDF rat glomeruli

(A-F) Double immunofluorescence staining of glomeruli of 34 wks old obese ZDF rats with nephrin and (A) clathrin heavy chain, (B) rab5, (C) cathepsin D, (D) p62, (E) CD2AP or (F) podocin. The antibodies used are listed in Supplemental Table S1. Scale bars: 50 μm.

Supplemental Figure S2. Nephrin and PACSIN2 colocalize at the plasma membrane with caveolin-1 and occasionally with clathrin light chain

(A-D) TIRF microscopy analysis of podocytes overexpressing clathrin light chain-eGFP (A, C) or caveolin-1-DsRedmonomer (B, D), and PACSIN2-mCherry (C) or PACSIN2-eGFP (D). In (A) and (B), podocytes were incubated in the presence of 516-647N for 20 min prior to fixation. TIRF microscopy reveals that nephrin and PACSIN2 colocalize regularly with caveolin-1 and occasionally with clathrin light chain (arrowheads). Mouse PACSIN2-mCherry and caveolin-1-DsRedmonomer were described in (1). Clathrin light chain-eGFP was subcloned into pEF-BOS vector as in (1). Scale bar: 10 μm.

Supplemental Figure S3. PACSIN2 knockdown increases the insertion of nephrin at the plasma membrane. A significant amount of internalized nephrin is recycled back to the plasma.

(A) Western blot showing overexpression of flag-PACSIN2 in podocytes. β-actin is used as a loading control. (B, C) Quantification of Western blots similar as in (A) reveals a 2-fold increase of PACSIN2 (B) without affecting nephrin levels (C). (D) Western blot of mouse podocyte lysates after transfection of scrambled or PACSIN2 siRNAs. (E) Quantification of Western blots similar as in (D) reveals that PACSIN2 siRNA-treatment decreased the level of PACSIN2 by 59%. (F) On-Cell Western analysis shows that knockdown of PACSIN2 increases the amount of nephrin inserted at the plasma membrane (n_{well}=54). Mouse podocytes expressing nephrin were transfected with ON-TARGET plus SMARTpool mouse PACSIN2 (L-045093-01-0005) or siCONTROL Non-Targeting Pool#2 (D-001206-14-05) siRNAs (Dharmacon, Lafayette, CO)

using Lipofectamine 2000 (Invitrogen, Carlsbad, CA) 16 h after plating and used for experiments after 48 h. (G, H) To confirm that internalized nephrin is recycled back to the plasma membrane, we performed qualitative immunofluorescence (G) and quantitative On-Cell Western (H) control experiments in which we added the 5-1-6 IgG to the culture medium of podocytes for 30 min, allowing internalization of IgG-labeled nephrin molecules. Thereafter, cells were acid stripped (1,15% acetic acid, 0.5 M NaCl, 4 min on ice) to remove the IgG bound to nephrin molecules still present at the plasma membrane, followed by incubation in culture medium without 5-1-6 IgG for 0-120 min to allow recycling of nephrin. Finally, a fluorescently labeled secondary IgG was applied without permeabilization to stain nephrin that was recycled back to the plasma membrane. With this approach, we observed that a significant amount of labeled, internalized nephrin was recycled back to the plasma membrane, reaching a peak of 15% 30 min after stripping (Supplemental Figure S3G, H). The nuclear marker DRAQ5 (ThermoFisher) was used for normalization in (H). In (H, n_{well}=33-54), * and # indicate that the statistical test was performed against no stripping or 0 min, respectively. Scale bar: 40 µm. Bars show the mean and error bars the standard deviation. The statistical analysis compares the mean of single wells from three experiments combined using Student's t-test. #p<0.05, **/##p<0.01, ****/####p<0.0001

Supplemental Figure S4. Rabenosyn-5-GFP overexpression does not change the expression level of nephrin or PACSIN2

(A) Western blot of rabenosyn-5-GFP overexpressing podocytes. β-actin is included as a loading control. (B-D) Quantification of Western blots similar as in (A) shows a 75% increase of total rabenosyn-5 (B) without affecting nephrin (C) or PACSIN2 (D) levels. Bars show the mean and error bars the standard deviation. Statistical significance is calculated using Mann-Whitney-U test. **p<0.01; ns, nonsignificant

Supplemental Figure S5. High glucose or palmitate do not change the expression levels of PACSIN2 and nephrin after 48 h treatment.

(A-C) Western blot of PACSIN2 and nephrin in podocytes treated with high glucose (A), palmitate (B) or both (C), as well as their respective controls. α-tubulin is included as a loading control. (D-E) Quantification of Western blots similar as in (A-C). Bars show the mean and error

bars the standard deviation. Statistical significance is calculated using Mann-Whitney-U test. ns, nonsignificant

Supplemental Table S1. List of antibodies used in the study.

The 5-1-6 IgG (3) was fluorescently labeled with NHS-ester Attodye 647N (Siegen, Germany), referred to as 516-647N.

Primary IgGs

Antigen	Host	Company/Sup. Reference
alpha-tubulin	mouse	Sigma-Aldrich, St. Louis, MO, USA
beta-actin	mouse	Sigma-Aldrich
cathepsin D	rabbit	Novus Biologicals, Littleton, CO, USA
CD2AP	rabbit	(2)
clathrin heavy chain	mouse	Calbiochem, San Diego, CA, USA
nephrin	guinea pig	PROGEN Biotechnik, Heidelberg, Germany
nephrin "5-1-6"	mouse	(3)
p62	guinea pig	PROGEN
PACSIN2 "P2B"	rabbit	Abgent, San Diego, CA, USA
PACSIN2 "P2P"	rabbit	(4)
podocin	rabbit	Sigma-Aldrich
rab5	rabbit	Cell Signaling Technology,Danvers, MA, USA
rabenosyn-5	rabbit	(5)

Secondary IgGs

Antigen	Host	Company/Sup. Reference
Alexa Fluor 594-anti rabbit	donkey	Molecular Probes, Eugene, OR, USA
Alexa Fluor 594-anti mouse	donkey	Molecular Probes
Alexa Fluor 488-anti mouse	donkey	Molecular Probes
Alexa Fluor 488-anti guinea pig	donkey	Molecular Probes
IRDye 800-anti mouse	goat	LI-COR Lincoln, NE, USA
IRDye 800-anti rabbit	donkey	LI-COR Lincoln
IRDye 680-anti mouse	donkey	LI-COR Lincoln
IRDye 680-anti guinea pig	donkey	LI-COR Lincoln

Supplemental Video S1. Nephrin is internalized in PACSIN2-eGFP positive sites.

Podocytes overexpressing PACSIN2-eGFP (green) and nephrin are incubated in the presence of 516-647N IgG (red). TIRF microscopy is used to observe the endocytosis of nephrin. Time is shown in seconds. Scale bar: 2 μm

Supplemental references

1. Senju, Y., Itoh, Y., Takano, K., Hamada, S., and Suetsugu, S. (2011) Essential role of PACSIN2/syndapin-II in caveolae membrane sculpting. *Journal of Cell Science* **124**, 2032-2040.

2. Lehtonen, S., Ora, A., Olkkonen, V. M., Geng, L., Zerial, M., Somlo, S., and Lehtonen, E. (2000) In vivo interaction of the adapter protein CD2-associated protein with the type 2 polycystic kidney disease protein, polycystin-2. *The Journal of Biological Chemistry* **275**, 32888-32893.

3. Topham, P. S., Kawachi, H., Haydar, S. A., Chugh, S., Addona, T. A., Charron, K. B., Holzman, L. B., Shia, M., Shimizu, F., and Salant, D. J. (1999) Nephritogenic mAb 5-1-6 is directed at the extracellular domain of rat nephrin. *The Journal of Clinical Investigation* **104**, 1559-1566.

4. Modregger, J., Ritter, B., Witter, B., Paulsson, M., and Plomann, M. (2000) All three PACSIN isoforms bind to endocytic proteins and inhibit endocytosis. *Journal of Cell Science* **113 Pt 24**, 4511-4521.

5. Navaroli, D. M., Bellve, K. D., Standley, C., Lifshitz, L. M., Cardia, J., Lambright, D., Leonard, D., Fogarty, K. E., and Corvera, S. (2012) Rabenosyn-5 defines the fate of the transferrin receptor following clathrin-mediated endocytosis. *Proceedings of the National Academy of Sciences of the United States of America* **109**, E471-80.